The final publication is available at

http://doi.org/10.1016/j.jcat.2017.06.014

Additional Information

Nature of active sites on UiO-66 and beneficial influence of water in the catalysis of Fischer esterification

Chiara Caratelli[1], Julianna Hajek[1], Francisco G. Cirujano[2], Michel Waroquier[1], Francesc X. Llabrés i Xamena[2], Veronique Van Speybroeck[1]*

[1]Center for Molecular Modeling (CMM), Ghent University, Technologiepark 903, B-9052 Zwijnaarde, Belgium
[2]Instituto de Tecnología Química, Universitat Politècnica de València, Consejo Superior de Investigaciones Científicas, Avda. de los Naranjos, s/n, 46022 Valencia, Spain

*Corresponding author. E-mail address: veronique.vanspeybroeck@ugent.be (V. Van Speybroeck)

Abstract

Zirconium terephthalate UiO-66 type metal organic frameworks (MOFs) are known to be highly active, stable and reusable catalysts for the esterification of carboxylic acids with alcohols. Moreover, when defects are present in the structure of these MOFs, coordinatively unsaturated Zr ions with Lewis acid properties are created, which increase the catalytic activity of the resulting defective solids. In the present work, molecular modeling techniques combined with new experimental data on various defective hydrated and dehydrated materials, allow to unravel the nature and role of defective active sites in the Fischer esterification and the role of coordinated water molecules to provide additional Brønsted sites. Periodic models of UiO-66 and UiO-66-NH₂ catalysts have been used to unravel the reaction mechanism on hydrated and dehydrated materials. Various adsorption modes of water and methanol are investigated. The proposed mechanisms are in line with experimental observations that amino groups yield a reduction of the reaction barriers, although they have a passive role in modulating the electronic structure of the material. Water has a beneficial role on the reaction cycle by providing extra Brønsted sites and by providing stabilization for various intermediates through hydrogen bonds.
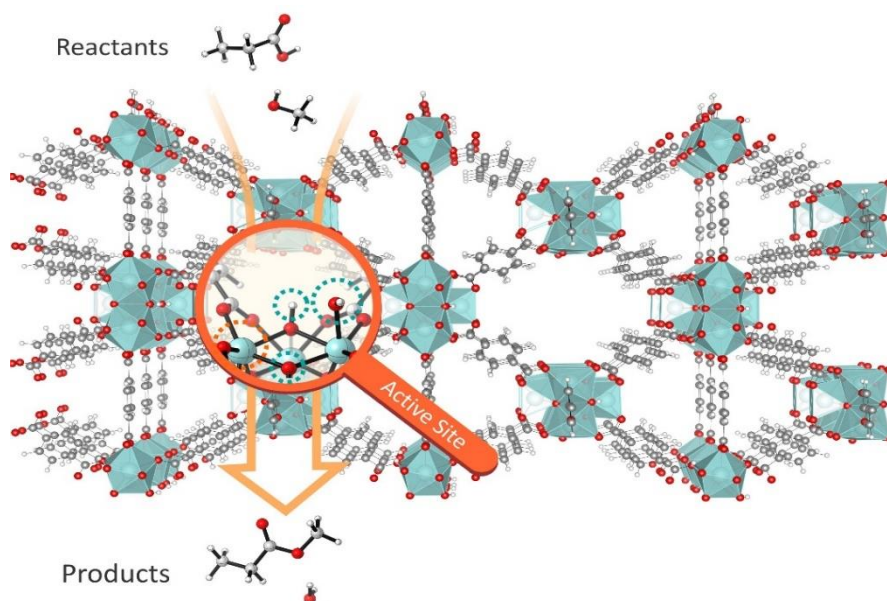
1. Introduction

The need of developing alternative energy sources is one of the world's highest priorities, as fossil sources are limited and their refinement and combustion contribute substantially to global warming. In this context, biofuels represent a possible solution to overcome the need of fossil fuels in sectors like transportation [1]. Biodiesel is a kind of biofuel that is obtained from organic feedstocks rich in lipids, such as vegetable oils and animal fats. It is similar in properties to petroleum diesel and represents a good renewable candidate that can already replace it in part. Its industrial production is currently performed via transesterification of triglycerides with low molecular weight alcohols, using strong Brønsted bases as homogeneous catalysts in anhydrous conditions [1, 2]. In this process, triglycerides, the main components of the feed, are converted into esters and glycerol is formed as a byproduct. This process, however, is very sensitive to the presence of Free Fatty Acids (FFA), which instead give water as a byproduct, leading to saponification and formation of emulsions in a basic environment. To avoid this problem, the feed must be purified from these components with quite expensive treatments contributing substantially to the production cost. An alternative approach consists in performing the esterification using strong inorganic acids as catalysts. A benefit of this process is that both the transesterification of triglycerides and esterification of free fatty acids can be catalyzed without unwanted side effects, allowing the production of biodiesel from low-cost feedstocks rich in FFA. However, these acids are highly corrosive and harmful to the environment. A way to overcome this issue consists in replacing mineral acids by solid heterogeneous acid catalysts as they could simultaneously convert both free fatty acids and triacylglycerols [3] while avoiding corrosion issues or dilution effects due to the generation of water. In addition, solid acid catalysts can be reused or applied in continuous processes, thus reducing the production cost. Besides biodiesel production, esterification is an important reaction also in the production of other derivatives of acids obtained by renewable sources, such as alkyl levulinates [1]. Therefore, the study of the esterification reaction mechanism and the development of good catalysts is of interest for a broad range of applications. So far, several suitable solid acid catalysts have been proposed, including zeolites, ion-exchange resins, and mixed metal oxides [4-6].

Few theoretical DFT studies on acid-catalyzed esterification of carboxylic compounds are available in literature. They all describe the reaction in gas phase or with small cluster models considering different pathways. Evidence was found that the reaction proceeds through a concerted mechanism [7, 8] although the literature is not always consistent in the description of the reaction mechanism [9]. The esterification of a generic carboxylic acid by methanol is schematically shown in **Scheme 1**.
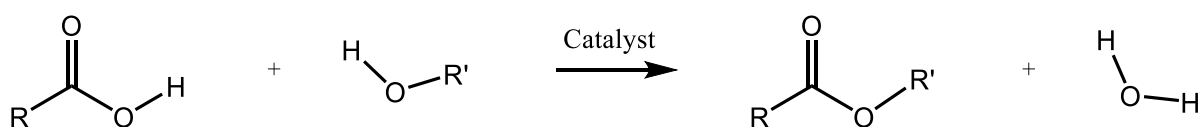
Scheme 1 Esterification of a generic carboxylic acid to an acid ester by alcohol

Recently, metal organic frameworks (MOFs) have attracted a lot of interest for their catalytic properties [10-14], among the wide range of other possible applications, such as drug delivery, gas and liquid sorption. MOFs are highly tunable materials, where metal or metal-oxo clusters are connected via organic linkers to form three dimensional crystalline porous networks. Their porosity, high metal content and tunability make MOFs outstanding candidates as catalysts. In particular, a Zr-terephthalate based MOF named UiO-66 [15] shows an exceptional stability [16-18] which allows its use in a wide range of thermal and chemical conditions. The key to its

stability lies in the high topological connectivity of the $[Zr_6O_4(OH)_4]^{12+}$ secondary building unit (SBU), which is connected with strong Zr-O bonds to 12 terephthalate (BDC) linkers. It is known that defects are present in the structure when linkers, metal ions or nodes are missing from the crystalline network [18]. Their amount can be tuned [19-22] without compromising the high stability of the material [23, 24]. However, the presence of defects in these materials can have a large impact on their catalytic properties.

Recently, defect engineering in UiO-66 has drawn a lot of attention from both a theoretical and experimental point of view [20, 23-28]. These defects can arise from one or more missing linkers and other building units, and their nature and spatial distribution are difficult to characterize experimentally. Nevertheless, their understanding is crucial and has been the subject of several studies on UiO-66 [23, 24, 26-32]. Defects increase the pore size, create room at metal centers for possible reactant adsorbates, and give rise to additional sites where molecules can be adsorbed. Therefore their presence is important for applications such as gas and liquid adsorption [33, 34]. In particular, it has been accepted that defects are responsible for the catalytic activity of this MOF [22, 24, 25], since missing linkers introduce coordinatively unsaturated Zr atoms in the solid, resulting in open Lewis acid sites. In particular, we refer to the extraordinary property of UiO-66 and variants to catalytically hydrolyze nerve agent simulants and thus to destruct chemical warfare agents [35, 36]. Furthermore, linkers can also be functionalized [37, 38], allowing a fine tuning of the catalytic behavior of the material [39]. UiO-66 has been shown to be a successful acid catalyst for the Fischer esterification [40, 41], with activities that are comparable and in some cases even superior to other homogeneous acid catalysts. In addition, the advantage of using a solid acid catalyst like UiO-66 is that the material is stable under reaction conditions and that it can easily be reused without significant loss of activity. In particular, it has been shown that the activity of UiO-66 in the esterification of levulinic acid (LA) and lauric acid increases with amino functionalization, but the role of these NH_2-substituents was not yet clear [40, 41]. However, recent experiments suggest an enhancing effect of the reaction due to the close position of the NH_2-group to the metal center, allowing a simultaneous activation of both LA and the alcohol. UiO-66-NH_2 behaves as a bifunctional acid-base catalyst as already proposed for cross-aldol condensation [42]. This feature has also been studied theoretically demonstrating the stabilizing effect of the amino-group in the condensation reaction without playing effectively an active role in the reaction [43].

The essential step to unravel the mechanism of the esterification reaction lies in understanding the nature of the active sites on defective UiO-66. It has been previously accepted that the key to the catalytic activity of UiO-66 lies in the presence and accessibility of Lewis acid sites, but recent studies point toward a more complex scheme involving additional Brønsted sites formed by water and hydroxyl groups coordinated to the Zr atoms [24, 25, 28, 31, 33, 44, 45]. Generally, because the structure possesses different potential catalytic centers, namely Lewis and Brønsted, a simple relation between the structure and the activity cannot easily be established.

In this work we go beyond the current state of the art in the theoretical exploration of (defective) UiO-66 materials as solid acid catalysts for the esterification reaction of propionic acid; being a representative model for a generic carboxylic acid, including the more interesting biomass derived FFAs and levulinic acid. We particularly want to understand how the presence of water may affect the catalytic activity on Zr-MOFs from a mechanistic point of view. First, the water coordination around the metal and its immediate impact on the nature of the active site center will be investigated theoretically. Second, the catalytic effect on the esterification reaction resulting from a dehydration of the MOF will be described. New experimental data performed on

different catalyst samples containing a varying number of linker vacancies showed the beneficial effect of water in line with the theoretical results. We show that the lowest activated mechanism takes place in a water environment creating Brønsted sites in the network of coordinated water molecules next to Lewis sites on the coordinatively unsaturated Zr atoms, arisen from the removal of linkers. Our results support the mechanism of a concerted bifunctional pathway providing a specific example of acid-base catalysis and this is in full agreement with experimental observations.

2. Methodology

Computational methods

All reactions studied in this work are investigated by means of static approaches using periodic models. The same methodology and levels of theory are used as employed in the study of aldol condensation reactions in a previous work of part of the authors [43]. Extended cluster calculations were used as a first guess to explore the different possibilities for adsorption of reactants and reaction pathways. However, in this work preference is given to periodic calculations as extended cluster calculations have the disadvantage that they are inadequate to correctly describe the environment surrounding the active site. Periodic calculations fully resolve this shortcoming. We made use of the periodic VASP (Vienna Ab Initio Simulation Package) code [46-50], applying the projector augmented wave approximation (PAW) [51] and the Γ-point approximation for the sampling of the Brillouin zone. The influence of k-points was tested on this system in a previous work, and a minimal effect on the electronic energy (~0.2 kJ/mol) was observed by increasing the sampling to a 2x2x2 Monkhorst-Pack mesh [43]. The structures were optimized within DFT-D3 with PBE as exchange-correlation functional [52, 53] and including Grimme D3 dispersion corrections [54, 55]. Energy cutoff for the plane waves was set to 700 eV, while the convergence threshold for the electronic self-consistent field (SCF) calculations was fixed to 10^{-5} eV. A Gaussian smearing of 0.025 eV was also included to improve convergence. The energies were then only refined for the reaction mechanisms with single point calculations at B3LYP-D3 level of theory [56-58].

The periodic unit cell of UiO-66 consists of four hexameric Zr-bricks following the crystallographic structure provided by Cavka et al. [15]. To make some metal sites accessible to guest molecules acting as reactants for potential reactions, at least two linkers should be removed from the entire unit cell. A rationalization on the different structures that can be generated by removing two linkers has been done in recent work of some of the present authors [23, 59]. There exist seven distinct classes of structures containing two linker vacancies. In the present study we select that configuration (type 6 in **Figure 2** of ref. [23]) which offers the best perspectives for guest intrusion through the channels to the coordinatively unsaturated Zr-surface. This particular defect structure is visualized in **Figure 1** where the two missing linkers in the 4-brick unit cell (blue) are clearly observed. The symmetry of this linker deficiency permits in reducing the dimension of the unit cell to two bricks (orange) with different coordination number 10 and 12. They are displayed in the right panel of **Figure 1**. This reduced cell represents a good compromise between computational cost and accuracy, as the reactants adsorbed on the active site are always separated from their periodic images by a Zr brick and have a minimal interaction with each other. The defective brick has two active sites A and B (see **Figure 1**). Reactions will be simulated

on site A while site B will not actively participate in the reaction. We refer to the ESI for further computational details.
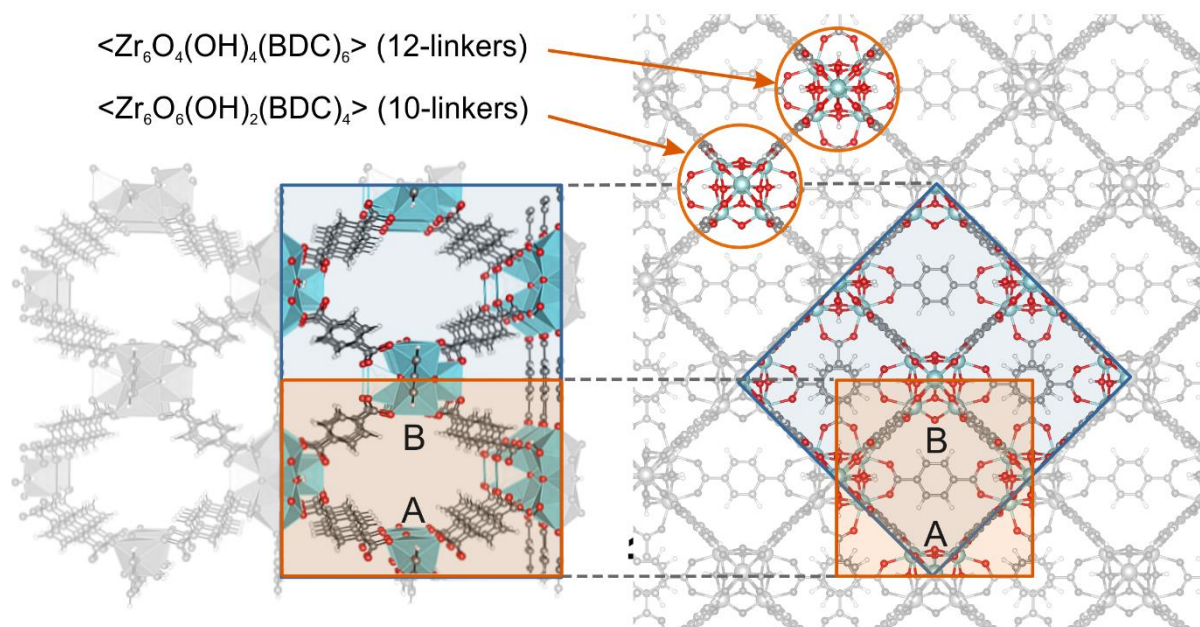
Figure 1: Representation of the unit cells containing the defect. In blue, the conventional 4-brick unit cell, in orange, the 2-brick unit cell used for the calculations. The two different bricks are highlighted in orange. The 10-fold coordinated brick has two terephthalate linkers missing, one at site A and one at the opposite site B.

While in an earlier paper of some of the authors [41] the esterification of free fatty acids has been experimentally simulated by lauric acid (with an alkyl chain of 12 C-atoms (n=12)), in the computational calculations the carboxylic acid is replaced by propionic acid with three carbon atoms. This is a seriously simplified model compound of a free fatty acid but it is large enough to investigate the reaction mechanism of the esterification reaction. A longer alkylic chain would add an excessive amount of degrees of freedom to the system, making the free energy surface of the adsorbate adduct much more complex and consequently would complicate the search for the most stable configuration. However, lauric acid or free fatty acids with longer chain lengths will not easily penetrate the pores of the UiO-66 material and reaction will take place at the surface and at the pore mouth. But as the active Zr-sites at the pore mouth are not structurally different from those in the interior (we refer the interested reader to the SM where an active surface site is constructed following the lines reported by Chizallet et al. [60, 61], it is plausible to assume that the employed model in this work to describe the esterification reaction mechanism is realistic. In the same context the alkyl chain of the acid can be regarded as passive and thus not affecting the reaction mechanism.

In order to account for the finite temperature, thermal corrections were performed from the frequency calculations. Using the in-house developed processing toolkit TAMkin [62] we calculated enthalpic and entropic contributions to the free energy barriers associated to each state at reaction conditions: temperature of 351 K and atmospheric pressure. A partial Hessian vibrational analysis approach was used [62], as it has been demonstrated [63] that this approximation does not affect substantially the entropy and enthalpy differences. The nature of stationary points was also verified by normal mode analysis using the partial Hessian frequency

calculations. Only positive eigenvalues were found for reactants and products (minima on the potential energy surface), while for transition states the presence of one negative eigenvalue associated with the normal mode along the reaction coordinate ensured that the system was in a first order saddle point. The atoms that were included in this partial Hessian frequency calculations are the reactants, the two Zr atoms, the two bridging μ_3-oxygen atoms of the active site, and the water molecules that are adsorbed. More details on various theoretical procedures to estimate the kinetics of heterogeneous catalyzed reactions may be found in references [64, 65].

Experimental methods

Synthesis of the MOFs
Several batches of UiO-66 and UiO-66-NH$_2$ solids were prepared using the procedure reported by Kandiah et al. [38]. 750 mg of ZrCL$_4$ and 740 mg of terephthalic acid (for UiO-66) or 800 mg of 2-amino terephthalic acid (for UiO-66-NH$_2$) were dissolved in 90 mL of DMF (Zr:ligand:DMF molar ratio of 1:1:220) and kept in a flask at 80°C without stirring for 12h, and at 100°C for other 24 h in an oil bath. The resulting material was recovered by filtration, then washed with fresh DMF. The solids were then washed three times by soaking in dichloromethane for 3 h. Finally, the solids were filtered and dried under vacuum. The high crystallinity and the structure of the materials was confirmed by X-ray diffraction (Phillips X'Pert, Cu, Kα radiation). MOFs were further characterized by thermogravimetric analysis (Mettler Toledo TGA/SDTA851e) and transmission electron microscopy (JEOL JEM-1010 operated at 100 kV) in order to determine linker deficiency and particle size, respectively. For further details on the synthesis of UiO-66, we refer to Cirujano et al. [40, 41].

General procedure for the esterifications
Esterification reactions of levulinic acid with ethanol were performed in a batch reactor at 78°C, where 1 mmol of acid and ethanol (0.6 mL, 15 mmol) were contacted with the MOF (0.018 mmol Zr). The reaction products were analyzed with GC-MS (Varian 3900) with a BP20(WAX) capillary column (15 m long, i.d. 0.32 mm), with dodecane as internal standard and comparing retention times with those of commercial standards.

3. Results and discussion

Molecular level characterization of defects - Water, methanol and acid coordination on the defective metal sites
In order to understand the reaction mechanism, it is crucial to have knowledge about the structure of the different active sites present on the material. Defects are generated during the synthesis, and the creation of a missing linker defect in the material can be imagined as a removal of one of the twelve negatively charged BDC^{2-} linkers from the [Zr$_6$O$_4$(OH)$_4$]$^{12+}$ brick. This produces a positive charge on the brick, which can be compensated either by removing a positively charged proton of the μ_3-OH groups of the oxoclusters (see **Scheme 2**), or - in the presence of water - by coordinating a negative species such as a hydroxyl group to one of the Zr atoms.
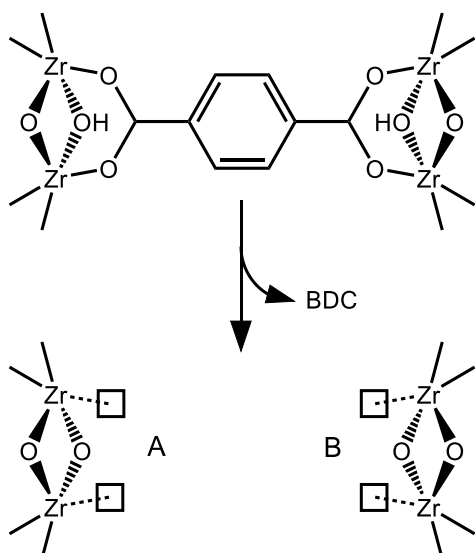
Scheme 2: Unsaturated sites upon removal of a terephthalate linker

Experimental determination of the nature of such defects on the molecular level is a very difficult task to accomplish. Single-crystal X-ray diffraction (SXRD) is a suitable tool to experimentally observe the presence of terminating hydroxyl groups and/or coordinating water molecules [26, 31]. In the work of Yaghi et al. [26] an extra hydroxide anion per defect site has been observed bringing the total of water molecules that can coordinate with a defective Zr-O-Zr site to three. In addition, it has been postulated that the charge compensating OH^- counterion upon removal of one linker is stabilized by a hydrogen bond with a neighboring μ_3-OH of the brick, while the two adjacent Zr atoms are capped with physisorbed water molecules. However, recent ab initio molecular dynamics simulations with water molecules moving in the pores of the UiO-66 material have shown that this state proposed by Yaghi does not correspond to a minimum on the potential energy surface [28, 45]. In the present work we did not succeed in reproducing it as an intermediate stationary state either. On the contrary configuration **3** of **Figure 2** with three water molecules coordinated to the defective Zr-O-Zr site goes over to a more stable configuration with the hydroxide ion coordinated to one of the Zr-atoms (complex **3'**).

Potentiometric acid-base titrations have been very recently applied as an alternative experimental technique to measure the number of defect sites in a MOF [25]. This technique is also useful to measure the Brønsted acidity or to trace the proton topology [66]. It helps to understand the role of the Brønsted acidity of the protons present on the inorganic nodes. Tuning of the chemistry of reactive groups such as hydroxyl groups on MOF nodes has become possible for the first time [67], whereby the formation of methoxy or ethoxy groups on node vacancy sites as intermediate states has been shown to be crucial for conversion between different structures of hydrogen bonded OH/OH_2 groups on the Zr_6-nodes. The various types of hydroxyl groups on the Zr_6-nodes have markedly different properties. The chemistry associated with these various face topology changes on the Zr_6 nodes has been investigated in ref. [67], and will be part of the discussion in this work.

Water coordination near the defective site can occur in several configurations which are all displayed in **Figure 2**. The active sites in the complex are not limited to Lewis acid sites. The unsaturated site formed after removal of a BDC linker (**Scheme 2**) is taken as the reference configuration R. The active site A contains two μ_3-oxygens bridging the Zr-atoms figuring as two Brønsted basic sites (reference configuration R in **Figure 2**).

7

The simplest state is chosen as reference and is displayed in the bottom of **Scheme 2**. The stability of all face topologies displayed in **Figure 2**, has been investigated with respect to this reference configuration R. In all calculations a hydrated node surface structure (site B, located at the opposite brick) has been consistently taken into consideration, allowing a comparative discussion on the coordination energies.

The coordination of one water molecule to one Zr-atom of the inorganic brick shields the Lewis acid character of the Zr-atom but the coordinated water molecule can act as an additional Brønsted acid site (configuration **1**). In all other structures different possible Lewis and Brønsted sites appear which may play a role in a catalytic reaction. The various sites are encircled in all structures displayed in **Figure 2**. The most stable configurations at the reaction temperature of 351 K are complexes with two or three water molecules. Configuration **2'** originates from a complex with two physisorbed water molecules on two adjacent Zr atoms (complex **2**). One water molecule immediately dissociates into a hydroxyl group adsorbed on one of the Zr-atoms and a proton adsorbed on the adjacent μ_3-oxygen, while the second water molecule is physisorbed on the other Zr atom. Structure **2'** forms a strongly stable configuration with a free energy difference of -94.4 kJ/mol compared to reference configuration **R** representing the unsaturated Zr site without water coordination. Adding a third water molecule yields a complex (configuration **3**) which is more stabilized than the complex with two coordinated water molecules (configuration **2**). Similarly as in the previous case, one water molecule dissociates with the OH⁻ counterion directly attached to one of the Zr-atoms, and the proton forming a μ_3-hydroxyl group, a second water molecule is coordinated to the adjacent Zr-atom, while the remaining water molecule is coordinated to the μ_3-hydroxyl group and the Zr-OH group. This configuration **3'** is slightly more stable than structure **2'** with two water molecules, but the difference is small (~4 kJ/mol), which can be ascribed to the seriously increasing entropy effects dominating the gain in enthalpy by the extra coordination. The position, orientation of the water molecules and the coordination energies of configuration **3'** are in agreement with what was observed by Vandichel et al. and Ling et al. [28, 45].

When reactant molecules (i.e., methanol and propionic acid) come into play, they can be hindered by the coordinating water molecules to access the active metal site, or the water can be displaced to make room for the incoming reactants, or the water molecules can form a complex with the reactants by means of hydrogen bonds. These complexes with reactants are considered in **Figure 3** and **4**. These states are consistently modeled on a unit cell where the two Zr atoms on the opposite active site generated by removal of a linker (site **B** in **Figure 1**) are hydrated (configuration **2'**). Analogous structures with the dehydrated site **B** are reported in the ESI (**Figure S3** and **S4**). Configuration **4** in **Figure 3** corresponds to the physisorbed complex with methanol on the Zr Lewis center (i.e., MeOH + configuration **R**). This configuration is found to be less stable than its chemisorbed structure with formation of a methoxide (configuration **4'**). With the presence of one water molecule, more stabilized methanol complexes are formed (configurations **5** and **5'**, coming from MeOH coordinated to configurations **1** and **1'**). We did not study the dynamics of the methanol substitution process, as done in ref. [67], but thermodynamically we found that structure **5'** is the most favorable with the substitution of one water molecule by one methanol molecule in **2'** and abstraction of the coordinated methanol proton to the terminating hydroxide.

Water in configuration **5'** can be removed and replaced by the acid as second reactant to form a stable reactive complex **9'**, displayed in **Figure 4**. In a hydrous environment methanol can even

indirectly coordinate with the Zr-center through a hydrogen bond with a terminal OH group. This complex **8** is even more stabilized (-60.9 kJ/mol).

In all complexes displayed in **Figure 4**, the acid is coordinated to the Zr-atom via its carbonyl oxygen. All the configurations considered are energetically favored (structures **6** to **9'**), but the presence of water in the environment is beneficial in the formation of stable complexes of the two reactants (acid + methanol) with the catalyst. The extra stabilization results from the formation of a hydrogen bonded adduct, e.g. in configuration **7**, with the μ_3-hydroxyl group present in UiO-66-H_2O (configuration **1'**).

Taken into account the results discussed so far, we propose structure **8** as reactive complex to study the esterification reaction of the acid by methanol in a hydrous environment, as it is the most stable adduct containing both reactant molecules, plus one water molecule that provides further stabilization through hydrogen bonding. The complex contains additional Brønsted acid and basic sites which may affect the esterification reaction of the acid with methanol, and forms a highly consistent structure of an adsorbed complex with all reactants in a hydrated UiO-66 material. It is taken as starting structure to test the reaction mechanism. On a dehydrated catalyst the situation is slightly different, water molecules are not present in the cavities of the material and a network of hydrogen bonded water molecules does not occur. Obviously, the most suitable configuration to start the reaction under anhydrous conditions is thus structure **9'**, formed upon propionic acid physisorption and dissociative chemisorption of methanol on the fully dehydrated defect site (configuration **R**). In following sections, the esterification reaction in both, hydrated and anhydrous conditions will be considered.
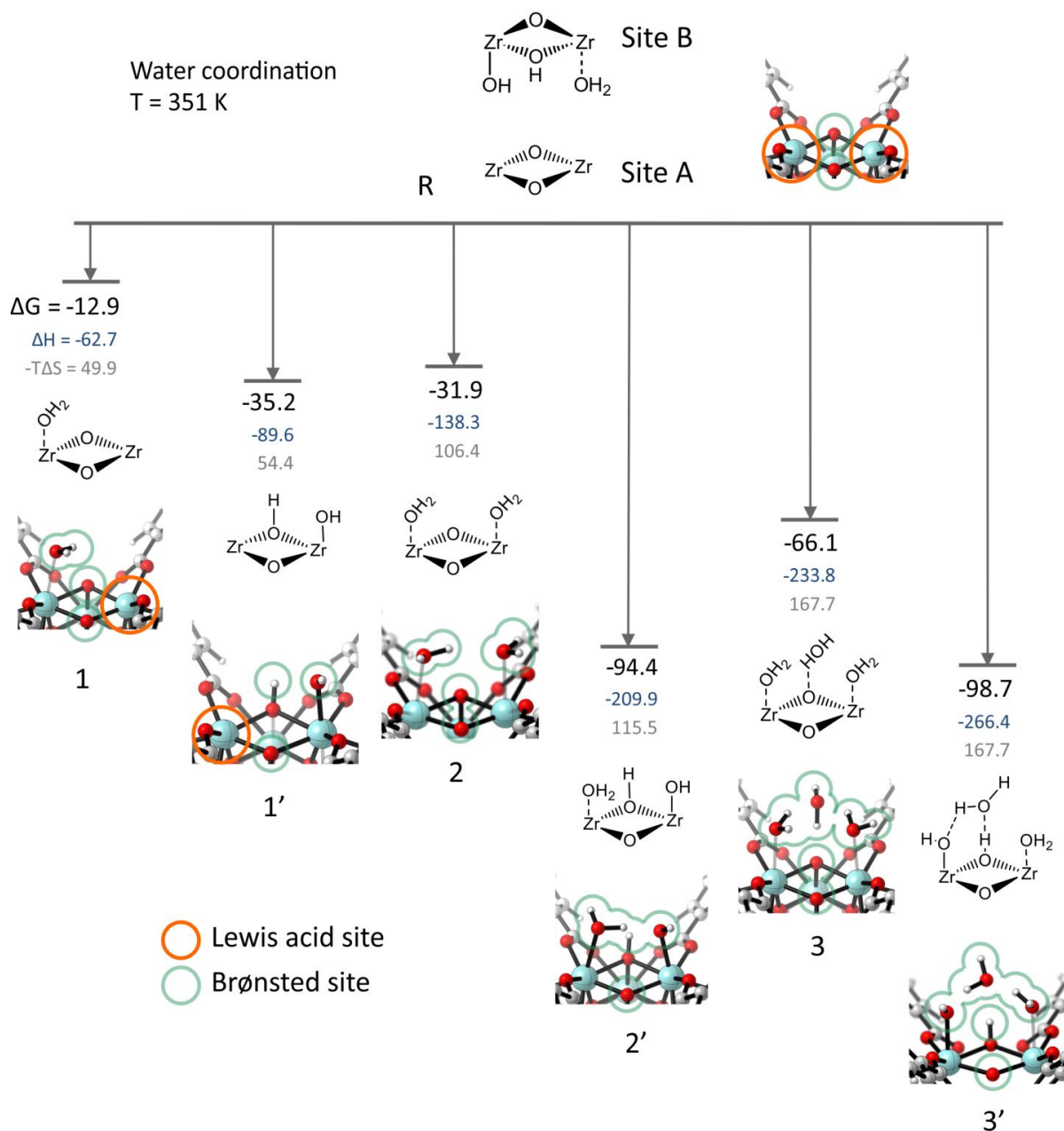
Figure 2: Coordination free energies at reaction temperature of 351 K of one, two and three water molecules at coordinatively unsaturated Zr-bricks in defective UiO-66 with respect to a water coordination free site (site **R**). The structure of the opposite site B corresponds with configuration **2'** with two water molecules and consistently used in all periodic calculations considered in the figure. Free energies (in black) are given in kJ/mol, and their decomposition into enthalpic ΔH (blue) and entropic -TΔS (grey) contributions. Energies are resulting from periodic calculations with PBE-D3 level of theory. In each configuration Lewis acid and Brønsted sites are indicated.
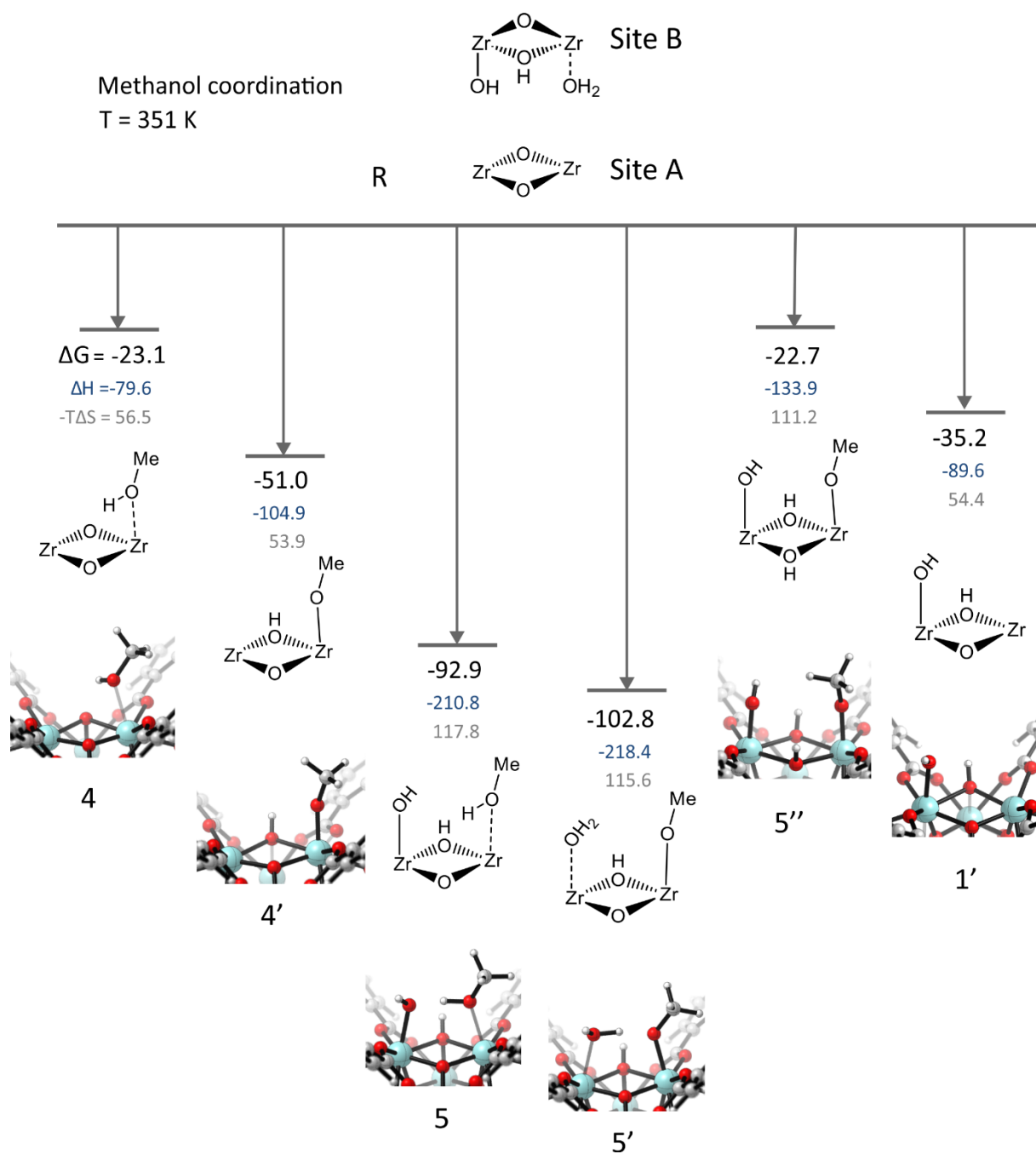
Figure 3: Coordination free energies at reaction temperature of 351 K of methanol at coordinatively unsaturated Zr-bricks in defective UiO-66 with respect to a water coordination free frame. The structure of the opposite site B corresponds with configuration **2'** with two water molecules and consistently used in all periodic calculations taken up in the figure. Free energies (in black) are given in kJ/mol, and their decomposition into enthalpic ΔH (blue) and entropic -TΔS (grey) contributions. Energies are resulting from periodic calculations with PBE-D3 level of theory.
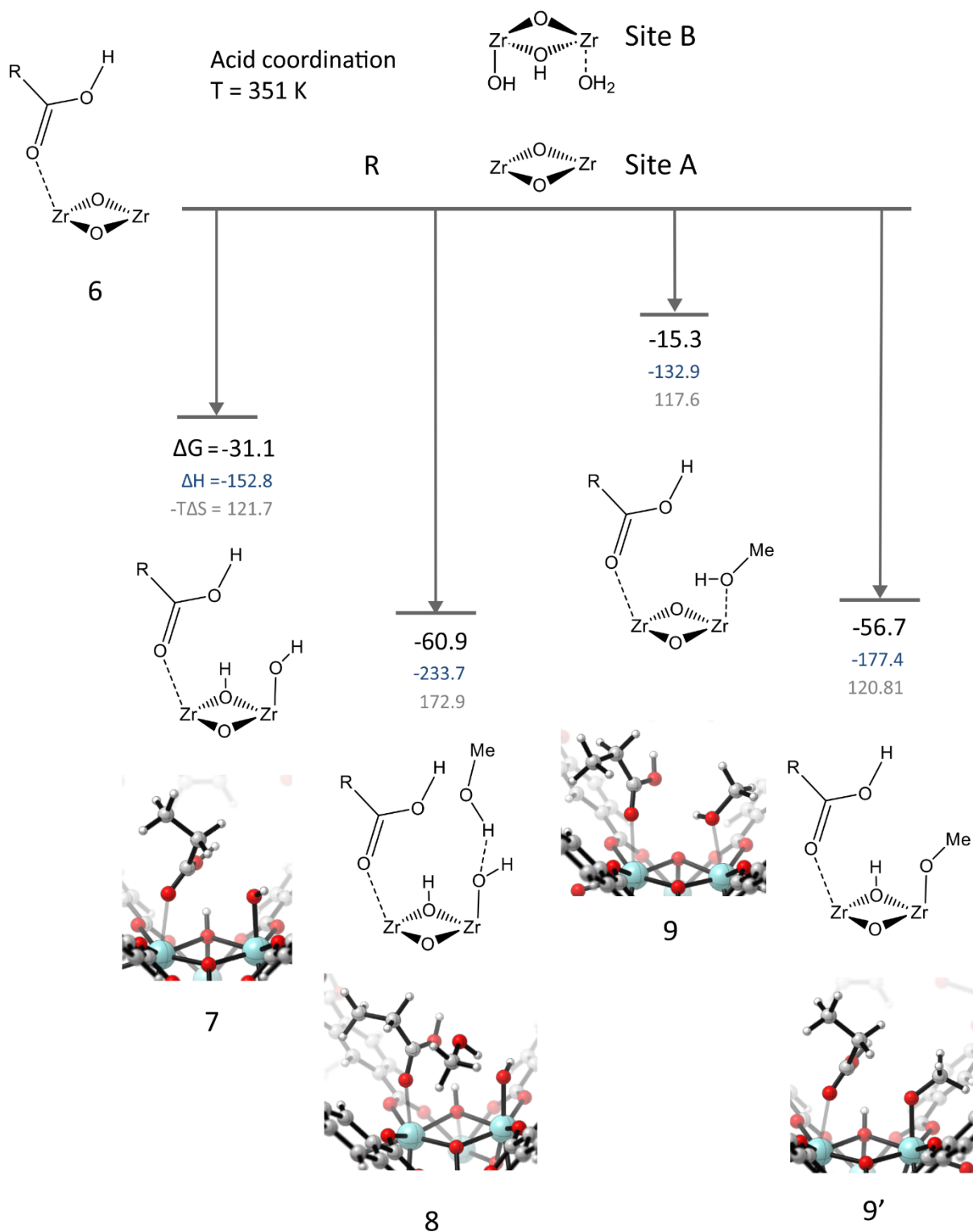
Figure 4: Coordination free energies at reaction temperature of 351 K of the propionic acid and coadsorption of methanol and water at coordinatively unsaturated Zr-bricks in defective UiO-66 with respect to a water coordination free frame. The structure of the opposite site B corresponds with configuration **2'** with two water molecules and consistently used in all periodic calculations taken up in the figure. Free energies (in black) are given in kJ/mol, and their decomposition into enthalpic ΔH (blue) and entropic -TΔS (grey) contributions. Energies are resulting from periodic calculations with PBE-D3 level of theory.

Reaction mechanism on hydrated brick

The coordination free energy diagrams in **Figures 2-4** clearly demonstrate that water molecules preferentially adsorb on the coordinatively unsaturated Zr-bricks in defective UiO-66, creating additional Brønsted sites which may assist in the esterification reaction. According to the proposed reaction mechanism and the catalytic effect of the defective UiO-66 material [40, 41], the adsorption of the carboxylic acid onto the Lewis Zr acid sites increases the electrophilic character of the carboxylic carbon atom. At the same time the presence of weak Brønsted basic sites in the close vicinity of the alcohol (formation of hydrogen bonded adducts) will increase the nucleophilic character of the oxygen of the alcohol, thus favoring the condensation with the activated carboxylic carbon of the acid. So far, the eventual beneficial influence of the presence of a water environment on the catalytic activity has not been tested theoretically. In a hydrated brick the most favorable complex for esterification is configuration **8** with the methanol hydrogen bonded with the water coordinated on the open metal site. The corresponding energy profile obtained starting from configuration **8** is shown in **Figure 5,** while the enthalpic and entropic contributions to the free energies of the states at different stages of the reaction are reported in **Table 1.**

The first transition state (**TS1**) is a concerted one, which corresponds to a deprotonation of methanol to the hydroxyl group, that acts as a Brønsted base, and to a simultaneous formation of a C—O bond between the oxygen of methanol and the carboxylic carbon. The free energy barrier for this first transition state is 28.9 kJ/mol with an almost equal enthalpic and entropic contribution. The post-transition state (configuration **8'**) is characterized by a tetrahedric intermediate coordinated to a Zr atom and a water molecule physisorbed on the adjacent Zr site. This intermediate has an almost similar free energy as the first reactive complex (configuration **8**) due to the extra-stabilization of a hydrogen bond with the μ_3-hydroxyl group. The second transition state (**TS2**) is characterized by an approaching of a hydroxyl group from the tetrahedric intermediate to the water molecule adsorbed on the other Zr atom. Simultaneously, a proton shifts from the water molecule to the hydroxyl group, so that water is formed as a byproduct. The energy barrier for this transition state is 30.6 kJ/mol, which is similar to the first energy barrier and makes it difficult to attribute a rate determining step for the final product formation. The reaction products (configuration **P**) are ester and water, but in a water environment the catalyst will remain in the strongly stabilized configuration **2'** and solely the ester will desorb from the catalyst whereas the water remains coordinated to the brick. The energy barrier for the reverse reaction is 91.7 kJ/mol, which allows part of the products to be converted again into the reactants, until a chemical equilibrium is attained. Indeed, it is also observed experimentally that this reaction is under thermodynamic control. The suggested mechanism characterized by relatively low free energy barriers overlays with experimental findings regarding the high activity of esterification on UiO-66 and shows a dual participation of conjugated Lewis acid and Brønsted sites, as suggested earlier [40, 41].
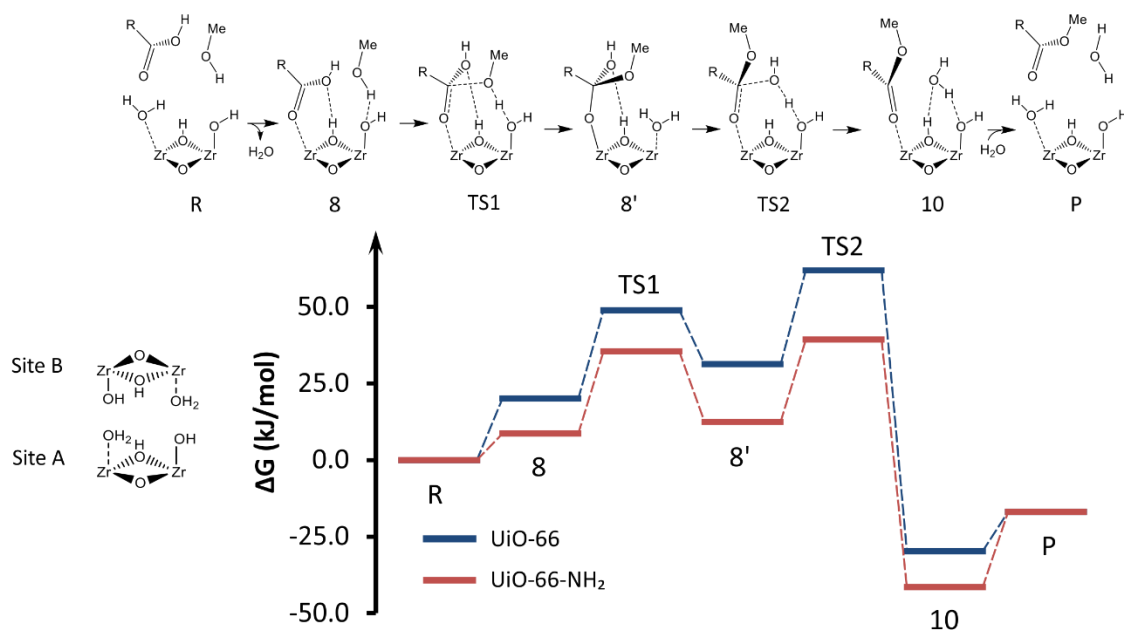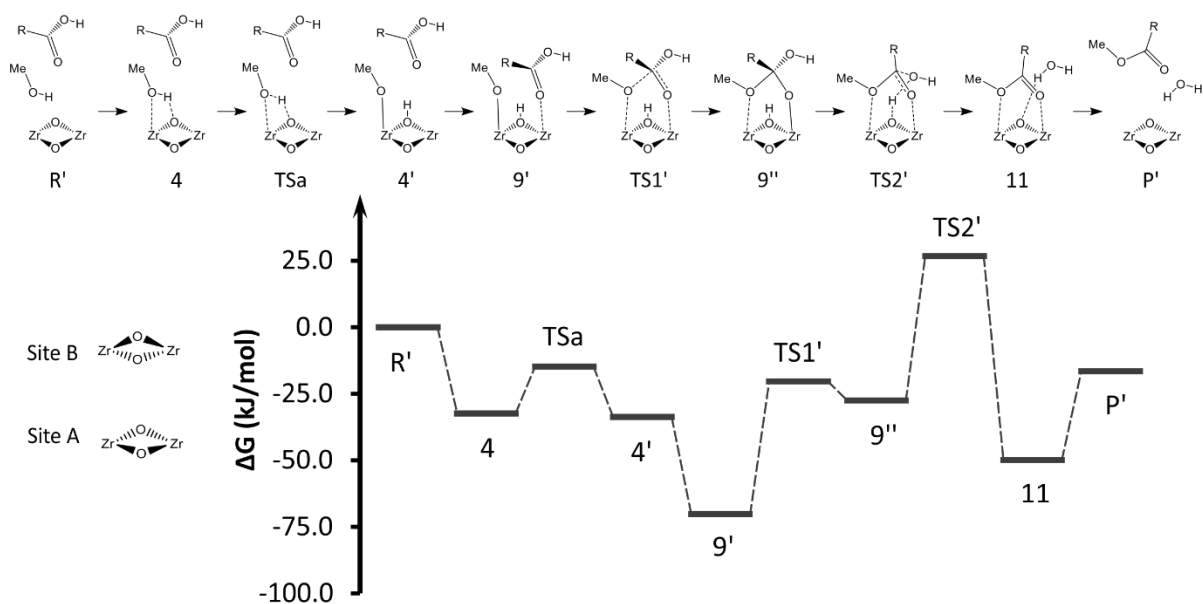
Figure 5: Mechanism and free energy profile for the esterification of propionic acid with methanol on a hydrated and defective UiO-66 material (blue), a hydrated defective UiO-66 material with amino functionalization of the BDC linkers (red), and on a dehydrated defective UiO-66 (black). Periodic calculations at B3LYP-D3//PBE-D3 level of theory, T=351 K. **R** corresponds with an empty frame with one linker defect and a pool with all reactants to guarantee mass balance. In **P** the defective Zr-brick is coordinated with two water molecules (configuration **2'**). **P'** corresponds to the empty frame with the ester as final product and remaining water molecules in gas phase.

Table 1: Free energy, enthalpic and entropic contributions in kJ/mol for the esterification of propionic acid with methanol on the hydrated, hydrated with NH_2-functionalisation and dehydrated UiO-66 material. Periodic calculations at B3LYP-D3//PBE-D3 level of theory, T= 351 K.

	Hydrated UiO-66					Hydrated UiO-66-NH_2			
	ΔG	$\Delta G^{\ddagger}$	ΔH	$-T\Delta S$		ΔG	$\Delta G^{\ddagger}$	ΔH	$-T\Delta S$
8	20.1		-32.3	52.4		8.7		-46.5	55.2
TS1	48.9	**28.9**	-17.9	66.8		35.5	**26.8**	-33.4	68.9
8'	31.3		-31.3	62.6		12.5		-55.0	67.5
TS2	62.0	**30.6**	-11.7	73.7		39.3	**26.9**	-31.9	71.2
10	-29.7		-87.0	57.3		-41.5		-98.3	56.8
P	-16.9		-20.1	3.2		-16.9		-20.1	3.2

	Dehydrated UiO-66			
	ΔG	$\Delta G^{\ddagger}$	ΔH	$-T\Delta S$
4	-32.3		-88.9	56.5
TSa	-14.8	**17.5**	-75.6	60.7
4'	-33.7		-88.2	54.5
9'	-70.1		-191.8	121.7
TS1'	-20.3	**49.8**	-161.0	140.7
9''	-27.5		-164.6	137.1
TS2'	26.7	**54.3**	-113.3	140.0
11	-49.8		-169.6	119.7
P'	-16.5		-19.8	3.2

Reaction mechanism in anhydrous conditions

Dehydration takes place after thermal activation of the catalyst. In an earlier paper of some of the authors [45] the mechanistic pathway for the dehydroxylation processes, that takes place at activation conditions (T>300°C) [18] of the various Zr-bricks present in defective UiO-66 material has been unraveled. Herein, experimental data, that will be discussed later in this paper, have been obtained after heat treatment of the material at a temperature of around 150°C. At this temperature the solvent water molecules are all removed, but the $[Zr_6O_6(OH)_2]^{10+}$ brick (structure **B'0** of ref. [45]) on which the reaction takes place remains still intact; i.e., no dehydroxylation of the brick takes places. The experimental results predict a drop of the catalytic activity after this heat treatment at 150°C (vide infra), and we will now demonstrate that, indeed, the esterification reaction on a dehydrated brick (reference configuration **R'** in **Figure 5**) in a water-free environment requires larger activation energies.

In the dehydrated brick the active sites are the uncoordinated Zr atoms, which are Lewis acid sites, and the μ_3-oxygen atom which is a Brønsted base. Methanol, present in large excess in the reactant mixture, is first physisorbed on one of the two unsaturated Zr centers (configuration **4**) with an adsorption energy of -32.3 kJ/mol at B3LYP-D3//PBE-D3 level of theory[1], In this complex the μ_3-oxygen atom represents a Brønsted basic site that facilitates the deprotonation of the methanol forming a methoxide, while the abstracted methanol proton forms a terminating μ_3–hydroxide (configuration **4'**). The methoxide complex is slightly thermodynamically favored with respect to its physisorbed configuration **4** and its formation requires a transition state **TSa** with a low free energy barrier of about 17 kJ/mol. Finally, the acid adsorbs on the adjacent free Zr-site, and a reactive complex (configuration **9'**) is formed ready to start the esterification. The reaction proceeds with the formation of the C—O bond between the carbonyl carbon of the acid and the oxygen of the deprotonated methanol. In this step the free energy barrier (**TS1'**) is 49.8 kJ/mol and is attributed to an enthalpic contribution of 30.8 kJ/mol and an entropic contribution of 19.0 kJ/mol. This barrier is significantly higher in these water-free conditions than in the previous case where water molecules are involved in hydrogen bonded adducts, creating weak Brønsted basic sites assisting in increasing the nucleophilic character of the oxygen of the deprotonated alcohol. Similarly to the proposed mechanism on the hydrated brick, we investigated whether a similar concerted mechanism of the deprotonation and O-C bond formation (**TS1** in the "hydrated" reaction path) is also valid on the dehydrated complexes, but this search failed. On the contrary, we found the following intermediate (configuration **9''**) which is very close in energy and geometry to the transition state (**TS1'**), with a slightly shorter bond distance between oxygen and carbon. Subsequently the intermediate complex **9''** loses a hydroxyl group that binds to the hydrogen adsorbed on the μ_3-oxygen atom (see reaction scheme in the bottom of **Figure 5**) to form a water molecule. This activated process also needs a high energy (barrier of transition state **TS2'** amounts to $\Delta G^{\ddagger}= 54.3$ kJ/mol). This implies that starting from the reactive complex **9'** a total barrier of around 96.8 kJ/mol should be overcome, which is more than two times higher than what is observed when water actively participates in the reaction.

The esterification reaction on a dehydrated Zr-brick gives always water as a byproduct that can be removed leaving the catalyst as a dehydrated Zr-brick (product **P'**). If this water molecule is not removed it disturbs the equilibrium of the reaction and will play a role in the further

---

[1] Please note that for the reaction free energy profile the level of theory has been increased from PBE-D3//PBE-D3 to B3LYP-D3//PBE-D3. It explains the difference in adsorption energy of complex 4 from -23.1 kJ/mol in **Figure 3** to -32.3 kJ/mol in **Figure 5**.

esterification as it will coordinate with the open metal sites and the subsequent reactions will come in competition with the reaction on a hydrated brick.

This dual behavior of the μ_3-oxygen atom was also observed in recent work by Hajek et al. on aldol condensation [43] and Oppenauer oxidation [68], where a deprotonation occurs on this site. The same site donates the proton back to form water in the last transition state. Therefore, also in this case we have a Brønsted site that acts as a base in a first step and as an acid in the next step. Note that in this pathway both Zr Lewis sites adsorb the reactants. We do not find a plausible pathway for the reaction that only makes use of the Lewis sites, therefore we conclude that the full catalytic effect is accomplished when the Brønsted sites are also taken into account.

The different kinetics of the esterification reaction in a water and a water-free environment require a more fundamental insight regarding the role of both Lewis and Brønsted sites present in the catalyst. It has been proposed that UiO-66 acted as a pure Lewis acid catalyst, given the Lewis acidity of the non-fully coordinated Zr atoms on the defect site. However, it is known that in other MOFs Brønsted groups such as hydroxyl, water, alcohol and acids can be coordinated to the metal sites on the bricks [69]. This acidity is difficult to characterize, as the acid sites are not homogeneous, and often lack an acid-base equilibrium. Moreover, because the structure possesses different potential catalytic centers - Lewis and Brønsted sites - a simple relation between the structure and the activity cannot easily be established. A compatible experimental technique to measure the Brønsted acidity or to trace the proton topology of MOFs in an aqueous environment is potentiometric acid-base titration. Using this technique three types of protons have been detected in UiO-66 material, attributed to: μ_3-OH, Zr-OH$_2$ and Zr-OH [66]. This picture is totally consistent with what we have proposed when removing a linker and replacing it by –OH$_2$ and –OH groups. A similar model has been proposed in recent computational studies of Ling and Slater [28] and Vandichel et al. [45] demonstrating that a proton is exchanged between the Zr-OH$_2$ and Zr-OH groups. This is in line with the proposed mechanism on the hydrated brick, as in the two transition states (TS1 and TS2) there is a proton exchange between reactants and the Zr-OH group, which in the first part of the reaction acts as a Brønsted base and in the second as a Brønsted acid. The reaction can be classified as some prototype of a dual acid-base catalytic reaction, where during the reaction Brønsted sites may alternatively switch of character. Their action works complementary to the Zr Lewis acid site whose role remains crucial in the esterification reaction. An actual theoretical study of the difference in acidity of the various protons would be very interesting but beyond the scope of the present paper.

Reaction mechanism with amino functionalization

One of the great advantages of MOFs is the easiness to functionalize the linkers and herewith to change the catalytic properties of the material. In order to understand the effect of the functional group substitution at the ligand benzene ring on the catalytic activity of the defective UiO-66 material, the esterification reaction was also investigated on the amino functionalized material, UiO-66-NH$_2$. It was originally speculated that amino groups would play an active role in the reaction. We investigated different pathways in which the amino group was actively involved, but no plausible mechanism was found. This brings us to the conclusion that the reaction needs Brønsted sites to be catalyzed, and that amino groups are not basic enough to deprotonate the reactants, which react preferentially with other basic sites, such as the Zr-OH group in the hydrated brick and the μ_3-oxygen atom in the dehydrated one. These results are in line with the

recent study of Hajek et al. on the aldol condensation reaction on the UiO-66 materials [43]. Therefore, the pathway that we have proposed previously for the hydrated brick of UiO-66, is still prevalent here with the amino functionalized material UiO-66-NH$_2$. However, even if the amino groups do not play a direct role in the reaction mechanism they could indirectly modulate the electronic structure of the framework and influence the reaction free energies. With an electron-donating substituent we may expect that the Lewis acid character of the coordinatively unsaturated neighboring Zr center decreases [39] and would lead to a decrease in the reaction rate. The lower Lewis acidity is reflected in longer distances between the carboxyl oxygen of the adsorbate and Zr in configuration **8** (Zr-O distance increases from 2.30 Å to 2.34 Å for UiO-66 and UiO-66-NH$_2$, respectively). However, the presence of a hydrogen bond network makes the electron modulation much more complex in this case, due to the interplay between the Lewis acid and the several Brønsted basic sites present in the hydrated complex, and leads overall to a slight increase in the reaction rate with amino functionalization. This is indeed what is observed here as different stabilization energies and barriers are obtained, compared with the amino-free material (see **Figure 5** and **Table 1**). The role of the amino group is passive and not visible in the reaction scheme. Nevertheless, a stronger adsorption of the reactants on the amino functionalized hydrated solid is noticed (configuration **8**) and systematically lower energy barriers, although not really spectacular. The stronger adsorption of the reactants on the UiO-66-NH$_2$ material is due to the formation of a network of hydrogen bonds which are not present in the pristine material (**Figure 6**, a), and to additional electronic effects. This extra stabilization affects all the states (intermediate, transition states and products), but the most striking effect is observed in the magnitude of the barrier (TS2) in the second reaction with the bond breaking between the carbonyl carbon and the oxygen of the leaving group. It lowers from 30.6 kJ/mol to 26.9 kJ/mol. The global effect of the amino functionalization is best expressed in the rate determining step which decreases by 11 kJ/mol, while the reaction is highly exothermic and under thermodynamic control. These results give rise to a higher catalytic effect that is indeed observed experimentally [40, 41]. Furthermore, amino groups provide additional sites where water can be adsorbed and form additional hydrogen bonds, as displayed in **Figure 6** (b). To summarize, in the proposed reaction mechanism, amino groups don't play an active role, but their presence induces a positive effect on the catalytic activity of the material, which completely agrees with the experimental observations. This effect was also observed in a recent theoretical work on aldol condensation [43]. The choice of an electron-withdrawing substituent such as -NO$_2$ will not enhance the esterification, despite the stronger Lewis acidity at the Zr-atom (see Supplementary Material). This is in line with our conclusion on the dual Lewis/ Brønsted character of the active site in the Fischer esterification.
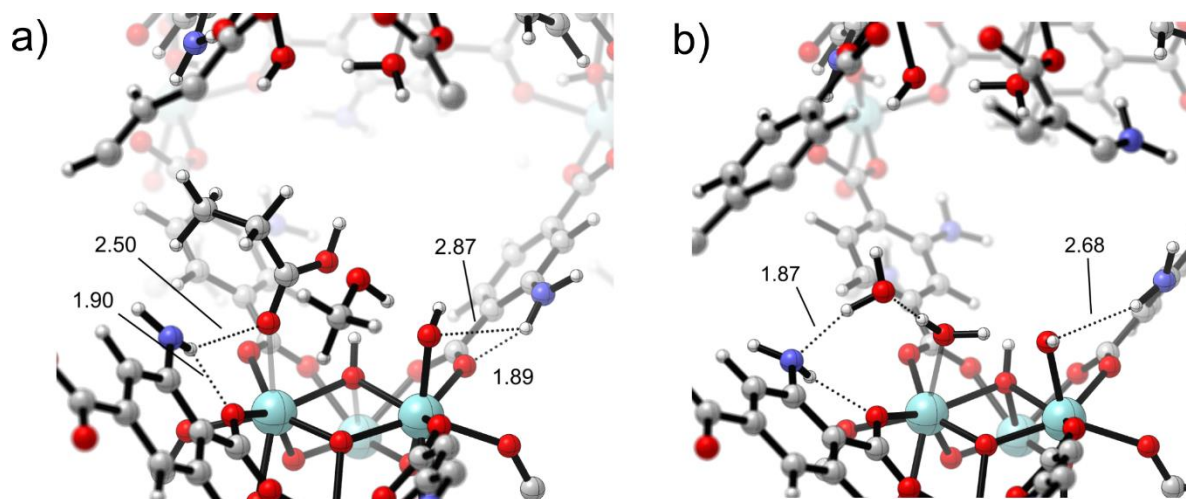
Figure 6: Network of hydrogen bonds between adsorbates and amino groups. a) reactive complex **8**, b) an additional water molecule present in solution.

Experimental results

The relevant role of water in the formation in UiO-66 materials of the active sites for esterification can be inferred experimentally by analyzing the thermograms of various samples containing different amounts of linker deficiencies. Indeed, TGA curves provide a means for evaluating the amount of missing linker defects of a solid, which can be calculated following the method proposed by Valenzano et al. [18]. In our previous paper on levulinic acid esterification over UiO-66-type materials [40], we showed that the use of a non-modulated synthesis procedure to prepare these materials (i.e., without the aid of auxiliary molecules, such as acetic acid), usually leads to materials which an amount of defects that can largely vary from one sample to another in a random way. In this way, we were able to prepare several samples with linker deficiencies ranging from 2.5 to 13.2% for UiO-66, and between 2.1 and 8% for UiO-66–NH_2. We made use of this large variability of defect content from sample to sample to establish a direct correlation between catalytic activity for esterification and the number of defects of the solid, in such a way that the catalytic activity was found to increase with the number of linker defects [40]. An almost 9-fold increment of the reaction rate constant (k) was observed on comparing the most defective (2.5% linker defects, k = 0.07 h^{-1}) to the less defective (13.2%, k = 0.61 h^{-1}) UiO-66 materials. Interestingly, by comparing the TGA curves of these UiO-66 samples, we have also noticed that a clear trend exists between the amount of linker vacancies and the total amount of physisorbed water of the solid (i.e., the weight lost between room temperature and 150ºC in the corresponding TGA curve (see **Figure 7**, left). Moreover, as the amount of linker defects in UiO-66 increases, water molecules are more strongly bound (i.e., desorbed at a higher temperature), as shown in **Figure 7**, right. This trend is clearly visible in the corresponding derivative of the TGA curves (red curves in **Figure S10** in ESI), in which the minima correspond to the inflection point of the first weight loss in the corresponding TGA curves. In contrast, in UiO-66-NH_2 water molecules are desorbed in general at higher temperatures than in UiO-66 with a similar concentration of defects: i.e., water molecules are more strongly bound. However, in UiO-66-NH_2 the desorption temperature does not seem to depend on the amount of missing linkers. Taken together, these results indicate that: i) the defects associated to linker vacancies increase the hydrophilic character of UiO-66, as already anticipated by Snurr and co-workers [33]; and ii) the presence of amino groups in the terephthalate linkers favors water adsorption, also in line with previous results by Walton and co-workers [70]. Therefore, these experimental findings give strong support

to the hypothesis of a direct participation of water molecules in the active (defective) sites for esterification, as suggested by our theoretical models. Moreover, they also offer a plausible explanation to understand the higher catalytic activity of UiO-66-NH$_2$ with respect to UiO-66. Even though our models do not predict a direct participation of the –NH$_2$ groups in any of the steps of the catalytic process, their presence clearly increases the amount of water adsorbed inside the pores and strengthens the interaction with the material, which results beneficial for the final catalytic activity.
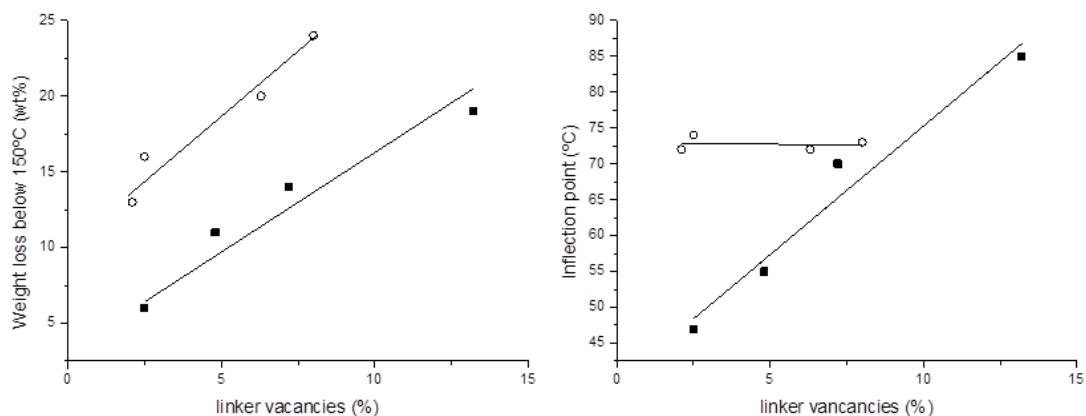
Figure 7: (Left) Weight lost between room temperature and 150ºC by UiO-66 (black squares) and UiO-66-NH$_2$ (white dots) as a function of the different amount of missing linker defects. (Right) Desorption temperature of physisorbed water (determined from the corresponding TGA derivative curves) as a function of missing linker defects for UiO-66 (black squares) and UiO-66-NH$_2$ (white dots). Both TGA and derivative TGA curves are shown in Figure S10 in ESI.
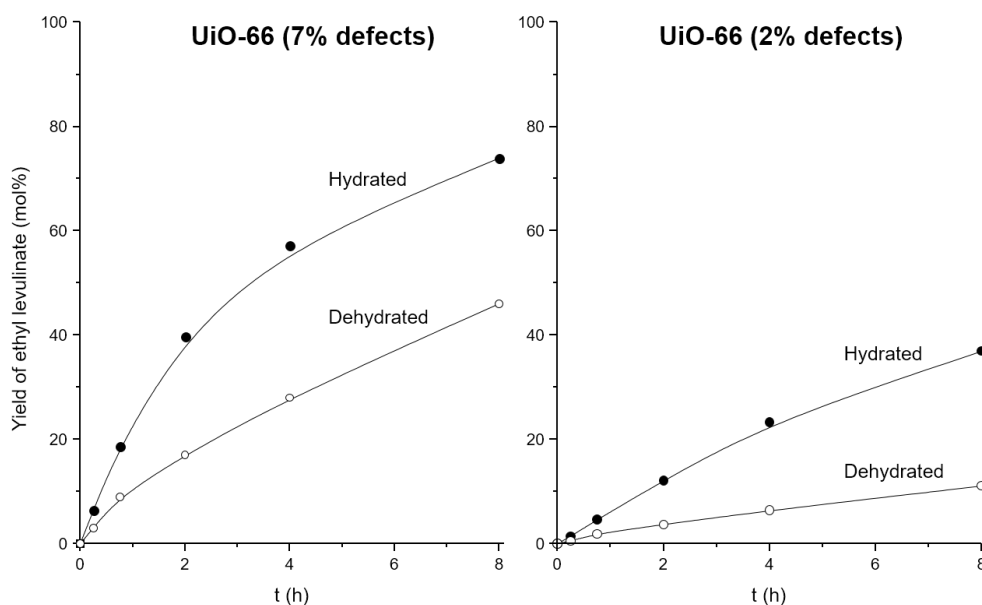
Figure 8: Time-conversion plots for esterification of levulinic acid (LA) with ethanol on UiO-66 with 7% defects (left) and 2% defects (right) when water is coordinated to the brick (black dots) and when the material is dehydrated (white dots).

An item that stirs a lot of experimentalists are the linker exchanges in MOFs. A recent perspective is given by Seth Cohen [71] and it is not excluded a priori that the carboxylic acid used in the esterification reaction exchanges with a terephthalate linker of the UiO-66 material. Linker exchange of terephthalate linkers by the carboxylate reaction substrates is in principle a feasible process that can take place during the reaction, leading to the creation of further defect sites

that could contribute to the catalytic process. Although we cannot completely rule out the occurrence of this phenomenon in the general case of any carboxylic acid, in the particular case of levulinic acid (LA) esterification we were not able to detect by 1H NMR and FTIR spectroscopy the presence of LA in the solid recovered after the catalytic experiment. Therefore, the amount of linker exchange (if any) should be certainly below the detection limits of these techniques. Indeed, if linker exchange of the pristine ditopic terephthalate linker by LA would take place to a significant extent, it would eventually lead to a severe reduction of the stability and crystallinity of the material. We have checked that the crystallinity of the material recovered after the reaction is virtually unchanged with respect to the fresh material (see Fig. S11 in the Supporting Information). Therefore, although ligand exchange cannot be totally ruled out for other carboxylic substrates, this should not be a significant process taking place during the reaction of LA with ethanol.

Finally, it is also possible to see experimentally a clear decrease of the catalytic activity of UiO-66 materials upon removal of physisorbed water molecules. To demonstrate this point, **Figure 8** shows the time-conversion plots obtained for the esterification of levulinic acid (LA) with ethanol catalyzed by two UiO-66 samples containing 7% (left part) or 2% (right part) missing linkers defects. The corresponding pseudo-first order reaction rate constants are k = 0.21 h^{-1} and 0.07 h^{-1} for samples with 7% and 2% missing linkers, respectively; following the trend observed in our previous work [40]. It is also observed in **Figure 8** that dehydration of the samples by thermal treatment at 150ºC (open symbols in both left and right parts) brings about a definite decrease of the catalytic activity of both UiO-66 samples; passing from 0.21 h^{-1} to 0.12 h^{-1}, and from 0.07 h^{-1} to 0.02 h^{-1}, for the samples containing 7% and 2% of defects, respectively. These results clearly reveal the relevant role of water in the catalytic activity of UiO-66 materials, which is a further support to our theoretical models and in complete agreement with the present findings.

The presence of defects in MOFs (both missing linkers and missing nodes) can eventually lead to an increase of the specific surface area and pore volume of the material, as compared to a pristine defect free material [72]. However, even if this type of defects would facilitate the diffusion of reactants throughout the pore system of the MOF, this would not translate into an improvement of the catalytic performance of the material for this particular reaction of the LA esterification with ethanol. However, we don't discard that other carboxylate substrates might eventually benefit for an increase of the material's porosity associated to missing nodes. We refer to the Supplementary Material for more details on this issue.

4. Conclusions

In this work we have investigated the mechanism of Fischer esterification of an organic carboxylic acid with methanol on UiO-66 and UiO-66-NH$_2$ with a linker deficiency. Particular attention has been drawn to the hydration state of the active sites on the materials. Theoretical modeling shows that in the most stable brick two water molecules are adsorbed on the defect site: one is chemisorbed as a Zr-OH group and a hydrogen on the μ_3-oxygen, while the other is physisorbed on the adjacent Zr. In the proposed mechanism, the carboxylic acid can displace the physisorbed water to coordinate with a Zr atom and react with methanol previously chemisorbed on the neighbor Zr site to form a methoxide. An alternative mechanism on the dehydrated brick and without the assistance of water was investigated, but the energy barriers were substantially

higher than in the previous case. This is in line with the experimental results reported herein that show a lowering in the catalytic activity upon dehydration of the material. Theoretical modeling confirms that the role of water molecules is crucial in the reaction, as water plays an active role as both Brønsted base and acid. As the role of the Zr Lewis acid centers is indispensable the proposed reaction mechanism is based upon a dual Lewis/Brønsted catalytic function. A positive effect of amino functionalization of the linkers was also observed, even though don't participate actively in the reaction mechanism. An indirect participation of the amino groups in increasing and strengthening water adsorption on the solid can be inferred from the analysis of the corresponding thermogravimetric curves, which would result beneficial for the formation and stabilization of the proposed active sites.

The model reaction studied in the present work between propionic acid and methanol can be taken as representative for other more relevant esterifications, in particular for the production of biodiesel from free fatty acids. Furthermore, water molecules could play an active role also in other reactions catalyzed by UiO-66 and other Zr based MOFs, such as MOF-808 and Nu-1000.

Finally, once more we want to emphasize the high potential of UiO-66 and its variants as catalyst due to its dual acid/base character by the appearance of Lewis and Brønsted sites working complementary to each other. Defective UiO-66 material is a prototype of how a MOF can be designed and composed such to fulfill all ingredients needed to construct such a combined Lewis/Brønsted network. The facile way to change the composition, topology of a MOF opens a lot of perspectives to use MOFs in catalytic applications.

5. Acknowledgements

References

[1] A. Corma, S. Iborra, A. Velty, Chemical Routes for the Transformation of Biomass into Chemicals, Chemical Reviews, 107 (2007) 2411-2502.

[2] G.W. Huber, S. Iborra, A. Corma, Synthesis of Transportation Fuels from Biomass: Chemistry, Catalysts, and Engineering, Chemical Reviews, 106 (2006) 4044-4098.

[3] N. Lerkkasemsan, N. Abdoulmoumine, L. Achenie, F. Agblevor, Mechanistic Modeling of Palmitic Acid Esterification via Heterogeneous Catalysis, Industrial & Engineering Chemistry Research, 50 (2011) 1177-1186.

[4] A.A. Kiss, A.C. Dimian, G. Rothenberg, Solid Acid Catalysts for Biodiesel Production —-Towards Sustainable Energy, Advanced Synthesis & Catalysis, 348 (2006) 75-81.

[5] E. Lotero, Y. Liu, D.E. Lopez, K. Suwannakarn, D.A. Bruce, J.G. Goodwin, Synthesis of Biodiesel via Acid Catalysis, Industrial & Engineering Chemistry Research, 44 (2005) 5353-5363.

[6] F. Ma, M.A. Hanna, Biodiesel production: a review1, Bioresource Technology, 70 (1999) 1-15.

[7] M. Vafaeezadeh, A. Fattahi, DFT investigations for "Fischer" esterification mechanism over silica-propyl-SO3H catalyst: Is the reaction reversible?, Computational and Theoretical Chemistry, 1071 (2015) 27-32.

[8] L. Zaramello, C.A. Kuhnen, E.L. Dall'Oglio, P.T. de Sousa Jr, DFT study of gas phase acid-catalyzed ethanolysis of butyric acid triglyceride, Fuel, 94 (2012) 473-479.

[9] T. Yu, H.-B. Chang, W.-P. Lai, X.-F. Chen, Computational study of esterification between succinic acid and ethylene glycol in the absence of foreign catalyst and solvent, Polymer Chemistry, 2 (2011) 892-896.

[10] A. Corma, H. García, F.X. Llabrés i Xamena, Engineering Metal Organic Frameworks for Heterogeneous Catalysis, Chemical Reviews, 110 (2010) 4606-4655.

[11] A. Dhakshinamoorthy, M. Alvaro, H. Garcia, Commercial metal-organic frameworks as heterogeneous catalysts, Chemical Communications, 48 (2012) 11275-11288.

[12] D. Farrusseng, S. Aguado, C. Pinel, Metal–Organic Frameworks: Opportunities for Catalysis, Angewandte Chemie International Edition, 48 (2009) 7502-7513.

[13] J. Lee, O.K. Farha, J. Roberts, K.A. Scheidt, S.T. Nguyen, J.T. Hupp, Metal-organic framework materials as catalysts, Chemical Society Reviews, 38 (2009) 1450-1459.

[14] P. Valvekens, F. Vermoortele, D. De Vos, Metal-organic frameworks as catalysts: the role of metal active sites, Catalysis Science & Technology, 3 (2013) 1435-1445.

[15] J.H. Cavka, S. Jakobsen, U. Olsbye, N. Guillou, C. Lamberti, S. Bordiga, K.P. Lillerud, A New Zirconium Inorganic Building Brick Forming Metal Organic Frameworks with Exceptional Stability, Journal of the American Chemical Society, 130 (2008) 13850-13851.

[16] Y. Bai, Y. Dou, L.-H. Xie, W. Rutledge, J.-R. Li, H.-C. Zhou, Zr-based metal-organic frameworks: design, synthesis, structure, and applications, Chemical Society Reviews, 45 (2016) 2327-2367.

[17] K. Leus, T. Bogaerts, J. De Decker, H. Depauw, K. Hendrickx, H. Vrielinck, V. Van Speybroeck, P. Van Der Voort, Systematic study of the chemical and hydrothermal stability of selected "stable" Metal Organic Frameworks, Microporous and Mesoporous Materials, 226 (2016) 110-116.

[18] L. Valenzano, B. Civalleri, S. Chavan, S. Bordiga, M.H. Nilsen, S. Jakobsen, K.P. Lillerud, C. Lamberti, Disclosing the Complex Structure of UiO-66 Metal Organic Framework: A Synergic Combination of Experiment and Theory, Chemistry of Materials, 23 (2011) 1700-1718.

[19] O.V. Gutov, M.G. Hevia, E.C. Escudero-Adán, A. Shafir, Metal–Organic Framework (MOF) Defects under Control: Insights into the Missing Linker Sites and Their Implication in the Reactivity of Zirconium-Based Frameworks, Inorganic Chemistry, 54 (2015) 8396-8400.

[20] G.C. Shearer, S. Chavan, S. Bordiga, S. Svelle, U. Olsbye, K.P. Lillerud, Defect Engineering: Tuning the Porosity and Composition of the Metal–Organic Framework UiO-66 via Modulated Synthesis, Chemistry of Materials, 28 (2016) 3749-3761.

[21] G.C. Shearer, S. Chavan, J. Ethiraj, J.G. Vitillo, S. Svelle, U. Olsbye, C. Lamberti, S. Bordiga, K.P. Lillerud, Tuned to Perfection: Ironing Out the Defects in Metal-Organic Framework UiO-66, Chemistry of Materials, 26 (2014) 4068-4071.

[22] F. Vermoortele, B. Bueken, G.l. Le Bars, B. Van de Voorde, M. Vandichel, K. Houthoofd, A. Vimont, M. Daturi, M. Waroquier, V. Van Speybroeck, Synthesis Modulation as a Tool To Increase the Catalytic Activity of Metal–Organic Frameworks: The Unique Case of UiO-66 (Zr), Journal of the American Chemical Society, 135 (2013) 11465-11468.

[23] S.M.J. Rogge, J. Wieme, L. Vanduyfhuys, S. Vandenbrande, G. Maurin, T. Verstraelen, M. Waroquier, V. Van Speybroeck, Thermodynamic Insight in the High-Pressure Behavior of UiO-66: Effect of Linker Defects and Linker Expansion, Chemistry of Materials, 28 (2016) 5721-5732.

[24] J. Canivet, M. Vandichel, D. Farrusseng, Origin of highly active metal-organic framework catalysts: defects? Defects!, Dalton Transactions, 45 (2016) 4090-4099.

[25] Y. Liu, R.C. Klet, J.T. Hupp, O. Farha, Probing the correlations between the defects in metal-organic frameworks and their catalytic activity by an epoxide ring-opening reaction, Chemical Communications, 52 (2016) 7806-7809.

[26] C.A. Trickett, K.J. Gagnon, S. Lee, F. Gandara, H.-B. Buergi, O.M. Yaghi, Definitive Molecular Level Characterization of Defects in UiO-66 Crystals, Angewandte Chemie-International Edition, 54 (2015) 11162-11167.

[27] M. Vandichel, J. Hajek, F. Vermoortele, M. Waroquier, D.E. De Vos, V. Van Speybroeck, Active site engineering in UiO-66 type metal–organic frameworks by intentional creation of defects: a theoretical rationalization, CrystEngComm, 17 (2015) 395-406.

[28] S.L. Ling, B. Slater, Dynamic acidity in defective UiO-66, Chemical Science, 7 (2016) 4706-4712.

[29] J.K. Bristow, K.L. Svane, D. Tiana, J.M. Skelton, J.D. Gale, A. Walsh, Free Energy of Ligand Removal in the Metal–Organic Framework UiO-66, The Journal of Physical Chemistry C, 120 (2016) 9276-9281.

[30] M.J. Cliffe, W. Wan, X. Zou, P.A. Chater, A.K. Kleppe, M.G. Tucker, H. Wilhelm, N.P. Funnell, F.-X. Coudert, A.L. Goodwin, Correlated defect nanoregions in a metal-organic framework, Nature Communications, 5 (2014) 4176.

[31] S. Øien, D. Wragg, H. Reinsch, S. Svelle, S. Bordiga, C. Lamberti, K.P. Lillerud, Detailed Structure Analysis of Atomic Positions and Defects in Zirconium Metal–Organic Frameworks, Crystal Growth & Design, 14 (2014) 5370-5372.

[32] D.S. Sholl, R.P. Lively, Defects in Metal–Organic Frameworks: Challenge or Opportunity?, The journal of physical chemistry letters, 6 (2015) 3437-3444.

[33] P. Ghosh, Y.J. Colon, R.Q. Snurr, Water adsorption in UiO-66: the importance of defects, Chemical Communications, 50 (2014) 11329-11331.

[34] H. Wu, Y.S. Chua, V. Krungleviciute, M. Tyagi, P. Chen, T. Yildirim, W. Zhou, Unusual and Highly Tunable Missing-Linker Defects in Zirconium Metal–Organic Framework UiO-66 and Their Important Effects on Gas Adsorption, Journal of the American Chemical Society, 135 (2013) 10525-10532.

[35] J.E. Mondloch, M.J. Katz, W.C. Isley Iii, P. Ghosh, P. Liao, W. Bury, G.W. Wagner, M.G. Hall, J.B. DeCoste, G.W. Peterson, R.Q. Snurr, C.J. Cramer, J.T. Hupp, O.K. Farha, Destruction of chemical warfare agents using metal–organic frameworks, Nat Mater, 14 (2015) 512-516.

[36] A.M. Plonka, Q. Wang, W.O. Gordon, A. Balboa, D. Troya, W. Guo, C.H. Sharp, S.D. Senanayake, J.R. Morris, C.L. Hill, A.I. Frenkel, In Situ Probes of Capture and Decomposition of Chemical Warfare Agent Simulants by Zr-Based Metal Organic Frameworks, Journal of the American Chemical Society, 139 (2017) 599-602.

[37] S.J. Garibay, S.M. Cohen, Isoreticular synthesis and modification of frameworks with the UiO-66 topology, Chemical Communications, 46 (2010) 7700-7702.

[38] M. Kandiah, M.H. Nilsen, S. Usseglio, S. Jakobsen, U. Olsbye, M. Tilset, C. Larabi, E.A. Quadrelli, F. Bonino, K.P. Lillerud, Synthesis and Stability of Tagged UiO-66 Zr-MOFs, Chemistry of Materials, 22 (2010) 6632-6640.

[39] F. Vermoortele, M. Vandichel, B. Van de Voorde, R. Ameloot, M. Waroquier, V. Van Speybroeck, D.E. De Vos, Electronic effects of linker substitution on Lewis acid catalysis with metal–organic frameworks, Angewandte Chemie International Edition, 51 (2012) 4887-4890.

[40] F. Cirujano, A. Corma, F.L. i Xamena, Conversion of levulinic acid into chemicals: Synthesis of biomass derived levulinate esters over Zr-containing MOFs, Chemical Engineering Science, 124 (2015) 52-60.

[41] F.G. Cirujano, A. Corma, F.X. Llabrés i Xamena, Zirconium-containing metal organic frameworks as solid acid catalysts for the esterification of free fatty acids: Synthesis of biodiesel and other compounds of interest, Catalysis Today, 257, Part 2 (2015) 213-220.

[42] F. Vermoortele, R. Ameloot, A. Vimont, C. Serre, D. De Vos, An amino-modified Zr-terephthalate metal-organic framework as an acid-base catalyst for cross-aldol condensation, Chemical Communications, 47 (2011) 1521-1523.

[43] J. Hajek, M. Vandichel, B. Van de Voorde, B. Bueken, D. De Vos, M. Waroquier, V. Van Speybroeck, Mechanistic studies of aldol condensations in UiO-66 and UiO-66-NH2 metal organic frameworks, Journal of Catalysis, 331 (2015) 1-12.

[44] J. Canivet, A. Fateeva, Y.M. Guo, B. Coasne, D. Farrusseng, Water adsorption in MOFs: fundamentals and applications, Chemical Society Reviews, 43 (2014) 5594-5617.

[45] M. Vandichel, J. Hajek, A. Ghysels, A. De Vos, M. Waroquier, V. Van Speybroeck, Water coordination and dehydration processes in defective UiO-66 type metal-organic frameworks, CrystEngComm, 18 (2016) 7056 - 7069.

[46] G. Kresse, J. Furthmuller, Efficient iterative schemes for ab initio total-energy calculations using a plane-wave basis set, Phys. Rev. B, 54 (1996) 11169-11186.

[47] G. Kresse, J. Furthmuller, Efficiency of ab-initio total energy calculations for metals and semiconductors using a plane-wave basis set, Computational Materials Science, 6 (1996) 15-50.

[48] G. Kresse, J. Hafner, Ab initio molecular dynamics for liquid metals, Phys. Rev. B, 47 (1993) 558.

[49] G. Kresse, J. Hafner, Ab initio molecular-dynamics simulation of the liquid-metal-amorphous-semiconductor transition in germanium, Phys. Rev. B, 49 (1994) 14251.

[50] G. Kresse, D. Joubert, From ultrasoft pseudopotentials to the projector augmented-wave method, Phys. Rev. B, 59 (1999) 1758-1775.

[51] P.E. Blochl, Projector augmented-wave method, Phys. Rev. B, 50 (1994) 17953-17979.

[52] J.P. Perdew, K. Burke, M. Ernzerhof, Generalized Gradient Approximation Made Simple, Physical Review Letters, 77 (1996) 3865.

[53] J.P. Perdew, K. Burke, M. Ernzerhof, Generalized Gradient Approximation Made Simple [Phys. Rev. Lett. 77, 3865 (1996)], Physical Review Letters, 78 (1997) 1396.

[54] S. Grimme, Accurate description of van der Waals complexes by density functional theory including empirical corrections, Journal of Computational Chemistry, 25 (2004) 1463-1473.

[55] S. Grimme, J. Antony, S. Ehrlich, H. Krieg, A consistent and accurate ab initio parametrization of density functional dispersion correction (DFT-D) for the 94 elements H-Pu, J Chem Phys, 132 (2010).

[56] A.D. Becke, Density-functional exchange-energy approximation with correct asymptotic behavior, Physical Review A, 38 (1988) 3098-3100.

[57] A.D. Becke, Density Functional Thermochemistry 3. The Role Of Exact Exchange, J Chem Phys, 98 (1993) 5648-5652.

[58] C.T. Lee, W.T. Yang, R.G. Parr, Development of the Colle-Salvetti Correlation-Energy Formula Into a Functional of the Electron-Density, Phys. Rev. B, 37 (1988) 785-789.

[59] A. De Vos, K. Hendrickx, P. Van Der Voort, V. Van Speybroeck, K. Lejaeghere, Missing Linkers: An Alternative Pathway to UiO-66 Electronic Structure Engineering, Chemistry of Materials, (2017).

[60] C. Chizallet, S. Lazare, D. Bazer-Bachi, F. Bonnier, V. Lecocq, E. Soyer, A.-A. Quoineaud, N. Bats, Catalysis of Transesterification by a Nonfunctionalized Metal−Organic Framework: Acido-Basicity at the External Surface of ZIF-8 Probed by FTIR and ab Initio Calculations, Journal of the American Chemical Society, 132 (2010) 12365-12377.

[61] C. Chizallet, N. Bats, External Surface of Zeolite Imidazolate Frameworks Viewed Ab Initio: Multifunctionality at the Organic−Inorganic Interface, The Journal of Physical Chemistry Letters, 1 (2010) 349-353.

[62] A. Ghysels, T. Verstraelen, K. Hemelsoet, M. Waroquier, V. Van Speybroeck, TAMkin: A Versatile Package for Vibrational Analysis and Chemical Kinetics, Journal of Chemical Information and Modeling, 50 (2010) 1736-1750.

[63] A. Ghysels, D. Van Neck, M. Waroquier, Cartesian formulation of the mobile block Hessian approach to vibrational analysis in partially optimized systems, J Chem Phys, 127 (2007) 164108.

[64] V. Van Speybroeck, K. De Wispelaere, J. Van der Mynsbrugge, M. Vandichel, K. Hemelsoet, M. Waroquier, First principle chemical kinetics in zeolites: the methanol-to-olefin process as a case study, Chemical Society Reviews, 43 (2014) 7326-7357.

[65] M. Waroquier, K. De Wispelaere, J. Hajek, S.M.J. Rogge, J. Van der Mynsbrugge, V. Van Speybroeck, Theoretical tool box for a better catalytic understanding, in: Nanotechnology in Catalysis: Applications in the Chemical Industry, Energy Development, and Environment Protection, 3 Volumes, Wiley-VCH, 2017.

[66] R.C. Klet, Y.Y. Liu, T.C. Wang, J.T. Hupp, O.K. Farha, Evaluation of Bronsted acidity and proton topology in Zr- and Hf-based metal-organic frameworks using potentiometric acid-base titration, Journal of Materials Chemistry A, 4 (2016) 1479-1485.

[67] D. Yang, V. Bernales, T. Islamoglu, O.K. Farha, J.T. Hupp, C.J. Cramer, L. Gagliardi, B.C. Gates, Tuning the Surface Chemistry of Metal Organic Framework Nodes: Proton Topology of the Metal-Oxide-Like Zr6 Nodes of UiO-66 and NU-1000, Journal of the American Chemical Society, (2016).

[68] J. Hajek, B. Bueken, M. Waroquier, D. De Vos, V. Van Speybroeck, The remarkable amphoteric nature of defective UiO-66 in catalytic reactions, ChemCatChem, (2017) DOI: 10.1002/cctc.201601689.

[69] J. Jiang, O.M. Yaghi, Brønsted Acidity in Metal–Organic Frameworks, Chemical Reviews, 115 (2015) 6966-6997.

[70] P.M. Schoenecker, C.G. Carson, H. Jasuja, C.J.J. Flemming, K.S. Walton, Effect of Water Adsorption on Retention of Structure and Surface Area of Metal-Organic Frameworks, Industrial & Engineering Chemistry Research, 51 (2012) 6513-6519.

[71] S.M. Cohen, The Postsynthetic Renaissance in Porous Solids, Journal of the American Chemical Society, 139 (2017) 2855-2863.

[72] M.R. DeStefano, T. Islamoglu, S.J. Garibay, J.T. Hupp, O.K. Farha, Room-Temperature Synthesis of UiO-66 and Thermal Modulation of Densities of Defect Sites, Chemistry of Materials, 29 (2017) 1357-1361.